

---

## A DUAL CLOSED-LOOP CONTROL SYSTEM FOR MECHANICAL VENTILATION

Fleur Tehrani, PhD,<sup>1</sup> Mark Rogers, BS, RCP, RRT,<sup>2</sup>  
Takkin Lo, MD,<sup>3</sup> Thomas Malinowski, BS, RCP, RRT,<sup>2</sup>  
Samuel Afuwape, PhD,<sup>2</sup> Michael Lum, BS, RCP, RRT,<sup>2</sup>  
Brett Grundl, RCP, RRT,<sup>2</sup> and Michael Terry, RCP, RRT<sup>2</sup>

---

Tehrani F, Rogers M, Lo T, Malinowski T, Afuwape S, Lum M, Grundl B, Terry M. A dual closed-loop control system for mechanical ventilation.

J Clin Monit 2004; 18: 111–129

**ABSTRACT. Objective.** Closed-loop mechanical ventilation has the potential to provide more effective ventilatory support to patients with less complexity than conventional ventilation. The purpose of this study was to investigate the effectiveness of an automatic technique for mechanical ventilation. **Methods.** Two closed-loop control systems for mechanical ventilation are combined in this study. In one of the control systems several physiological data are used to automatically adjust the frequency and tidal volume of breaths of a patient. This method, which is patented under US Patent number 4986268, uses the criterion of minimal respiratory work rate to provide the patient with a natural pattern of breathing. The inputs to the system include data representing CO<sub>2</sub> and O<sub>2</sub> levels of the patient as well as respiratory compliance and airway resistance. The *I:E* ratio is adjusted on the basis of the respiratory time constant to allow for effective emptying of the lungs in expiration and to avoid intrinsic positive end expiratory pressure (PEEP). This system is combined with another closed-loop control system for automatic adjustment of the inspired fraction of oxygen of the patient. This controller uses the feedback of arterial oxygen saturation of the patient and combines a rapid stepwise control procedure with a proportional-integral-derivative (PID) control algorithm to automatically adjust the oxygen concentration in the patient's inspired gas. The dual closed-loop control system has been examined by using mechanical lung studies, computer simulations and animal experiments. **Results.** In the mechanical lung studies, the ventilation controller adjusted the breathing frequency and tidal volume in a clinically appropriate manner in response to changes in respiratory mechanics. The results of computer simulations and animal studies under induced disturbances showed that blood gases were returned to the normal physiologic range in less than 25 s by the control system. In the animal experiments under steady-state conditions, the maximum standard deviations of arterial oxygen saturation and the end-tidal partial pressure of CO<sub>2</sub> were  $\pm 1.76\%$  and  $\pm 1.78$  mmHg, respectively. **Conclusion.** The controller maintained the arterial blood gases within normal limits under steady-state conditions and the transient response of the system was robust under various disturbances. The results of the study have showed that the proposed dual closed-loop technique has effectively controlled mechanical ventilation under different test conditions.

**KEY WORDS.** Mechanical ventilation, closed-loop control, work of breathing, multiple data feedback, oxygen.

From the <sup>1</sup>Department of Electrical Engineering, California State University, Fullerton, CA 92831, U.S.A., <sup>2</sup>Department of Respiratory Care, and the <sup>3</sup>Medical Intensive Care Unit, Loma Linda University Medical Center, Loma Linda, CA 92354, U.S.A.

Received 14 May, 2003, and in revised form 10 Feb, 2004. Accepted for publication 20 Feb, 2004.

Address correspondence to F.T. Tehrani, College of Engineering and Computer Science, California State University, Fullerton, P.O. Box 6870, Fullerton, CA 92834-6870, U.S.A.  
E-mail: ftehrani@fullerton.edu

---

## INTRODUCTION

In the past few decades there have been many advances in mechanical ventilators to enhance their features and make them more responsive to individual patient's needs. But

despite all these advances, most ventilators are mainly open-loop control devices. The added features of ventilators that have enhanced their flexibility have also contributed to their complexity.

Closed-loop ventilators can offer many advantages to patients as well as clinicians. These machines have the capability of providing more effective and flexible ventilatory treatment to patients with less complexity than traditional mechanical ventilators. The idea of closing the loop in mechanical ventilators is not new and a number of researchers have presented different closed-loop techniques for these machines since the mid 1950s [1–13]. In most of the techniques presented, however, only one variable, either the volume of expired CO<sub>2</sub> or the end-tidal partial pressure of CO<sub>2</sub> ( $P_{\text{etCO}_2}$ ) was used to adjust the output of the mechanical ventilator. Using CO<sub>2</sub> as a single control variable does not provide sufficient physiological information to the controller and can mask respiratory problems. This deficiency was remedied by incorporating several important variables in the control procedure in one of the techniques for closed-loop mechanical ventilation [10]. In this technique CO<sub>2</sub> and O<sub>2</sub> levels of the patient as well as respiratory compliance and airway resistance data are used to control the outputs of the ventilator. In this system, both tidal volume and the rate of breathing are adjusted automatically to minimize the respiratory work rate on the basis of a hypothesis by Otis et al. [14]. The rationale is to stimulate spontaneous breathing by providing a naturally comfortable breathing pattern to the patient on the ventilator. This technique, which was originally patented under US Patent 4986268, was later used in an article by a different group of workers [11].

In the present study, the closed-loop technique for automatic adjustment of the rate and tidal volume of breaths by using multiple data [10] has been combined with another closed-loop control technique for automatic adjustment of the inspired fraction of oxygen,  $F_{\text{IO}_2}$ . Supplemental oxygen treatment commonly accompanies mechanical ventilation to achieve stable and sufficient oxygenation. In current methods of mechanical ventilation,  $F_{\text{IO}_2}$  is manually controlled. The frequency of the manual adjustments depends on the severity of the patient's conditions and can become quite cumbersome for acutely ill patients. Several different techniques have been developed to control  $F_{\text{IO}_2}$  automatically [15–23]. In these techniques, feedback of arterial partial pressure of oxygen,  $P_{\text{aO}_2}$  [15], or transcutaneous oxygen pressure,  $P_{\text{tO}_2}$  [16], or arterial oxygen saturation measured by pulse oximetry,  $S_{\text{pO}_2}$  [17–23] has been used to control the level of  $F_{\text{IO}_2}$ . The aim has been to prevent hypoxemia as well as hyperoxemia and to minimize exposure to high levels of  $F_{\text{IO}_2}$ . In a recent technique developed for this purpose, two different control algorithms were combined to optimize the performance of the controller [22–23]. A

fast stepwise control mechanism and a less rapid fine-tuned control algorithm were combined in this technique. This oxygen control system demonstrated a significantly shorter response time to disturbances in oxygen balance of the patient as compared to the previous techniques. In this study, this system has been combined with the above-mentioned closed-loop control technique for the ventilator.

The ventilation controller uses  $P_{\text{etCO}_2}$  and  $S_{\text{pO}_2}$  of the patient, as well as respiratory compliance and airway resistance data, to automatically adjust the rate and depth of breathing. The respiratory work rate is minimized in this process and the  $I:E$  ratio is adjusted to allow for effective emptying of the lungs in expiration. Minimization of the respiratory work rate reduces the load on the respiratory muscles and stimulates natural spontaneous breathing. This, in turn, could have important implications in reducing the weaning time from the mechanical ventilator. The adjustment of the  $I:E$  ratio in accordance to breathing rate and respiratory mechanics, prevents gas trapping in lungs and development of intrinsic PEEP. The  $F_{\text{IO}_2}$  controller provides an effective and rapid response to oxygen disturbances. Using the  $F_{\text{IO}_2}$  controller, hypoxemia is corrected robustly while hyperoxemia is minimized and oxygen toxicity is prevented [22, 23].

While the  $F_{\text{IO}_2}$  controller is quite effective in oxygen control of the patient, it does not help the other aspects of ventilation such as adjustment of ventilation in response to CO<sub>2</sub>, respiratory work rate minimization, or prevention of gas trapping in the lungs. Combination of the two closed-loop control systems results in more effective and robust control of arterial blood gases, stimulates spontaneous breathing, and prevents the build up of intrinsic PEEP. Compared to previous techniques, the system presented in this paper includes the original aspects of utilizing multiple data in control of mechanical ventilation, as well as respiratory work rate minimization. The overall closed-loop system is tested by using computer simulations, mechanical lung studies, and animal experimentation.

---

## METHODS AND MATERIALS

---

### *Description of the control system*

Figure 1 shows the schematic diagram of the control system in this study. The digital processor detects and processes  $P_{\text{etCO}_2}$  and  $S_{\text{pO}_2}$  of the patient which are measured by using breath-by-breath capnography and pulse-oximetry. This data, together with the airway resistance and respiratory compliance data of the patient are used to calculate control signals for the signal generator and timing control circuit, which in turn generates control signals for the

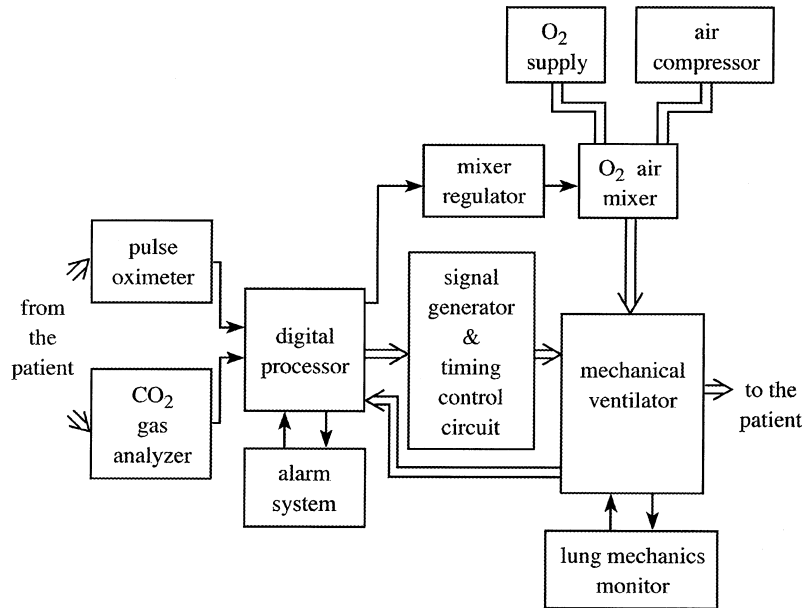


Fig. 1. The schematic diagram of the dual closed-loop control system.

ventilator. The  $S_{pO_2}$  data is further processed to calculate and generate a control signal for the oxygen mixer that controls the concentration of oxygen in the inspired gas of the patient for every breath. The digital processor uses two algorithms; the ventilation control program and the  $F_{IO_2}$  control program.

#### The ventilation controller

The input data provided to the closed-loop controller for mechanical ventilation represent arterial partial pressures of carbon dioxide and oxygen ( $P_{aCO_2}$ ,  $P_{aO_2}$ ), respiratory elastance,  $K'$ , airway resistance,  $K''$ , metabolic rate ratio, MRR, and the barometric pressure,  $P_b$ . Some of these variables must be measured whereas others can be stored in the software. In the experiments of this study,  $P_{etCO_2}$  and  $S_{pO_2}$  were measured for every breath by using capnography and pulse-oximetry. Data representative of  $P_{aCO_2}$  and  $P_{aO_2}$  were derived from these measurements for each breath whereas the values of airway resistance and respiratory elastance were monitored and inputted to the controller. The values of MRR and  $P_b$  were stored in the software.

The digital processor in the ventilation controller processes the input data on a breath-by-breath basis to determine the required ventilation and the breathing frequency of the patient. A flow-chart of the sequence of steps performed by the ventilation controller is shown in Figure 2. As can be seen, at the start of the flow-chart, after having set up the input and the output ports in step 1, initial values for

ventilation and the breathing frequency are provided to the output ports of the microprocessor in step 2. The alarm, coupled with one of the output ports is reset in step 3. Values representing the difference between  $P_{aCO_2}$  and  $P_{etCO_2}$ , the positive end expiratory pressure (PEEP), and  $P_b$  are read from the input ports or from the memory (if stored in the software) in step 4. Also, if dead space volume is measured, the data is read at this point. The respiratory compliance ( $1/K'$ ), and the airway resistance ( $K''$ ) values are also read in step 4, if they are not continuously monitored. In step 5, the program routine is held for the interval of the first breath (specified in step 2 by the initial value of the breathing frequency). Next, a program loop is started in step 6. Once the loop is entered, the values of  $P_{etCO_2}$  and  $S_{aO_2}$  are read from the input ports in step 7. In the next step, the values of respiratory compliance and airway resistance are read from the input ports, if the values of these variables are continuously monitored.

The next step shown at 9 is to calculate the values of patient's  $P_{aCO_2}$  and  $P_{aO_2}$ . These are calculated according to the following equations:

$$P_{aCO_2} = P_{etCO_2} + K_1 \quad (1)$$

$$P_{aO_2} = (-\ln[1 - (S_{pO_2})^{0.5}]/0.046) + CF \quad (2)$$

The symbols used in the equations are also defined in the Glossary. In Equation (1),  $K_1$  represents the difference between  $P_{aCO_2}$  and  $P_{etCO_2}$ . This value is measured in advance and entered in the software in step 4. Depending on

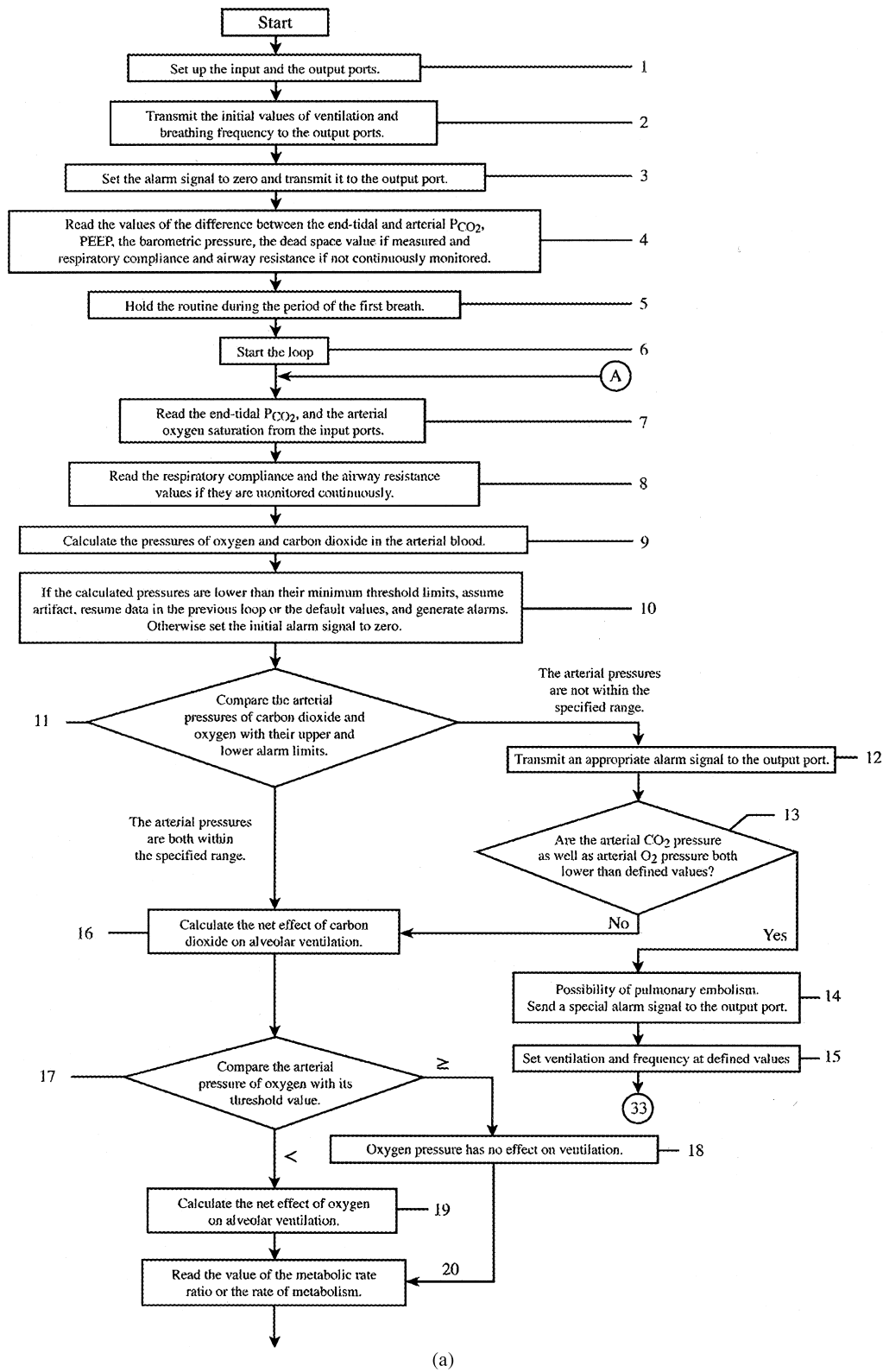


Fig. 2. Flow-chart of the algorithm for the closed-loop ventilation controller.

(Continued on next page)

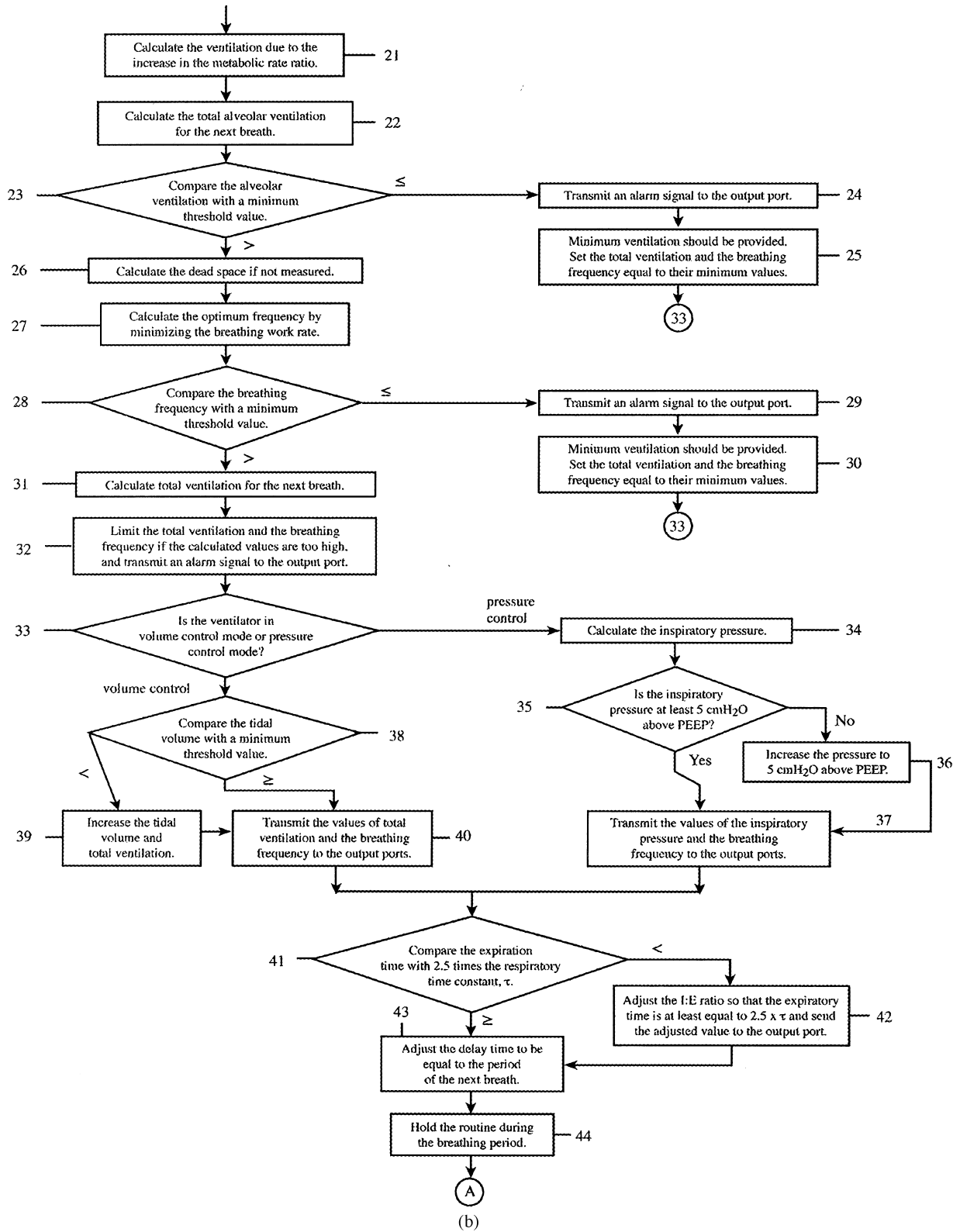


Fig. 2. (Continued)

the patient's conditions, the desired  $P_{aCO_2}$  of the patient can be set by appropriate adjustment of  $K_1$ . Equation (2) is based on the blood hemoglobin dissociation curve [24]. CF in this equation is an added correction factor that can be adjusted by the medical personnel to shift and correct  $P_{aO_2}$  based on the patient's blood pH level. If the patient's blood pH is in the normal range (i.e. 7.45–7.55), CF is set to zero. If the desired blood pH for the patient deviates from the normal range, CF needs to be adjusted (3.5 mmHg per 0.1 change in pH) [25].

After  $P_{aCO_2}$  and  $P_{aO_2}$  are calculated in step 9, they are compared to their minimum threshold limits in step 10 to detect any artifacts. If either of them is lower than its minimum threshold limit, an artifact is assumed, data in the previous loop for the corresponding partial pressure (or a default value if in the first loop) is resumed, and an alarm is generated. This is done in order to prevent provision of too high or too low ventilation to the patient due to erroneous measurements of  $P_{etCO_2}$  or  $S_{pO_2}$ . This is particularly important in regard to  $S_{pO_2}$  data, which may be subject to considerable noise due to artifact. This feature of the algorithm prevents the erroneous measurements of  $S_{pO_2}$  and  $P_{etCO_2}$  from having significant effect on  $F_{IO_2}$  and ventilation.

In step 11, the calculated  $P_{aCO_2}$  and  $P_{aO_2}$  values are compared to upper and lower alarm limits (the lower alarm limits at this step are different from those used to detect artifact in the previous step). If either of the pressures is outside the specified range (these ranges can be defined for different patients), an appropriate signal is generated and provided to the alarm unit via an output port as shown in step 12. If the calculated values of  $P_{aCO_2}$  and  $P_{aO_2}$  are both lower than the minimum alarm limits, the controller detects the possibility of a drastic change in the physiological dead space, such as due to pulmonary embolism, and sends a special alarm signal in step 14. In this case, predefined ventilation and frequency values are provided by the controller in step 15 and the routine is transferred to step 33. If both  $P_{aCO_2}$  and  $P_{aO_2}$  are not found to be below their lower alarm limits simultaneously in step 13, the step illustrated in 16 is next performed. In 16, if  $P_{aCO_2}$  is too low, the net effect of  $CO_2$  on ventilation is set to zero. Otherwise, the net effect of  $CO_2$  concentration on ventilation requirements is calculated according to the following equation:

$$V_C = C_1 P_{aCO_2} - C_2 \quad (3)$$

where  $V_C$  is the ratio of alveolar ventilation as the net effect of  $CO_2$  to the resting value of ventilation,  $C_1$  is the sensitivity factor of the controller to  $CO_2$ , and  $C_2$  is a constant. Equation (3) is based on multiple factor theory in control of respiration [10, 26]. In the present study,  $C_1$  was set at 0.405 and  $C_2$  was tuned at 13.0.

Next, as illustrated at 17,  $P_{aO_2}$  is compared to a threshold value of 104 mmHg. If the value of  $P_{aO_2}$  is greater than or equal to this threshold value, the effect of oxygen on ventilation is zero (step 18), and program control passes to step 20. If, on the other hand, the value of  $P_{aO_2}$  is less than the threshold value, then step 19 is performed and the net effect of  $P_{aO_2}$  on ventilation requirement is calculated according to the following equation [10, 26]:

$$V_O = (4.27 \times 10^{-9})(104 - P_{aO_2})^{4.9} \quad (4)$$

where  $V_O$  is the ratio of alveolar ventilation as the net effect of oxygen to the resting value of ventilation. In step 20, the rate of metabolism or the metabolic rate ratio (rate of metabolism/basal rate of metabolism) is read by the controller. This value is either read from the memory or from an input port. The metabolic rate ratio, MRR, is set equal to 1 and stored in the software in this study. The next step, illustrated in 21, is to calculate the effect of increasing MRR on ventilation. The following equation is used to calculate the net effect of MRR on ventilation [10, 27]:

$$V_M = 0.988(MRR - 1) \quad (5)$$

where  $V_M$  is the ratio of alveolar ventilation as the net effect of increase in MRR to the resting value of ventilation. In the next step, illustrated in 22, total alveolar ventilation for the next breath is calculated according to the following equation [10, 27]:

$$V_A = (V_A \text{ at rest})(V_C + V_O + V_M) \quad (6)$$

where  $V_A$  is the alveolar ventilation in l/min. Next, as shown in 23, the calculated value of  $V_A$  is compared to a minimum threshold value. If  $V_A$  is less than or equal to the threshold value, ventilation and breathing frequency are set to a predefined minimum in 25. Thereafter, program control turns to step 33 of the loop. If, however, in step 23, the value of  $V_A$  is determined to be greater than the minimum threshold value, then step 26 is performed. In step 26, the patient's physiologic dead space is determined. This value is either measured initially and entered in step 4 as mentioned earlier, or is calculated based on a patient model described by the following equations in step 26 [10, 27]:

$$V_D = 0.1698 V_A / 60 + C_3 \quad (7)$$

$$V_{Dt} = V_D + V_{ED} \quad (8)$$

where  $V_D$  is the dead space,  $V_{ED}$  the added dead space due to the tubes and connections to the ventilator and  $V_{Dt}$  the total dead space volume in liters. The parameter  $C_3$  in this equation depends on the type and conditions of the patient.

For normal adults, it is set to 0.1587 [27] and for infants equal to  $2.28 \times 10^{-3}$  l [28].

As illustrated in step 27, the next step is to calculate the optimum frequency for the next breath. This is determined on the basis of minimum work rate criterion. This is done in order to minimize the respiratory load and to stimulate natural breathing. The following equation, which is a modified version of the equation derived by Otis et al. [14], has been used to calculate the optimum breathing frequency to minimize the work rate of breathing [10]:

$$f = \frac{-K' V_D + \sqrt{(K' V_D)^2 + (4K' K'' \Pi^2 V_{AR} V_D)}}{2K'' \Pi^2 V_D} \quad (9)$$

where  $f$  is the optimum breathing frequency in breaths/s,  $V_{AR}$  the alveolar ventilation in l/s ( $V_{AR} = V_A/60$ ),  $K'$  the respiratory elastance (reciprocal of respiratory compliance) in  $\text{cmH}_2\text{O}/\text{l}$  and  $K''$  the airway resistance in  $\text{cmH}_2\text{O}/\text{l}/\text{s}$ .

Next, as shown in step 28, frequency ( $f$ ) is compared with a minimum threshold value. If the value of  $f$  is less than or equal to the threshold value, ventilation and frequency are set to minimum in step 30 and program control thereafter turns to step 33. If, however, the value of  $f$  is greater than the minimum threshold value, the next step, 31, is performed. In 31, total ventilation is calculated according to the following equation [10]:

$$V_E = V_A + 60f V_{Dt} \quad (10)$$

where  $V_E$  represents total ventilation in l/min. In step 32, total ventilation and frequency are compared to their upper limit values. If they happen to be too high, their values are limited and an alarm is sent to an output port.

In step 33, the mode of operation of the ventilator is checked. If it is in the pressure control/assist mode, the inspiratory pressure is calculated in 34 by using the respiratory elastance (reciprocal of compliance) value:

$$P_m = K' V_T + \text{PEEP} \quad (11)$$

where  $P_m$  is the inspiratory pressure in  $\text{cm H}_2\text{O}$ ,  $K'$  the respiratory elastance in  $\text{cmH}_2\text{O}/\text{l}$ , and  $V_T$  the tidal volume in l given by [10]:

$$V_T = V_A/60f + V_{Dt} \quad (12)$$

In the next step,  $P_m$  is compared with PEEP. If it is not at least 5  $\text{cm H}_2\text{O}$  above PEEP, its value is increased as a safety measure to avoid gas trapping, and the next step in 37 is performed. As illustrated in step 37, at this stage two digital signals representing  $P_m$  and  $f$  for the next breath are transmitted to the assigned output ports. The maximum limit of  $P_m$  is set in the ventilator by the medical personnel.

If in step 33, the ventilator is found to be in the volume control (VC)/assist mode, the step in 38 is performed. In this step, as shown,  $V_T$  is calculated by using Equation (12) and compared with a minimum threshold value of  $V_{\min} = V_{Dt} + V_D$ . If  $V_T \geq V_{\min}$ , the program control turns to step 40. Otherwise,  $V_T$  and correspondingly  $V_E$  is increased as an additional safety measure in step 39, and then the step 40 is performed.

In step 40, as shown, two digital signals representing  $V_E$  and  $f$  for the next breath are transmitted to the assigned output ports. In the next step 41, another safety measure is performed to avoid gas trapping in the lungs. In this step, the expiratory time is compared with the respiratory time constant. The minimum inspiratory time is set at 20% of the breath period. The minimum breath period cannot be shorter than five times the respiratory time constant,  $\tau$ , which is the ratio of airway resistance to respiratory elastance ( $K''/K'$ ). In step 41, if the expiratory time is shorter than  $2.5\tau$ , the  $I:E$  ratio is adjusted in step 42 to allow for effective emptying of the lungs in expiration and the next step 43 is then performed. If, however, the expiratory time is found to be longer or at least equal to  $2.5\tau$  in step 41, step 42 is skipped and 43 is followed.

In step 43, a delay interval is adjusted to be equal to the period of the next breath and the program is held for this interval in step 44. After the hold time expires, control turns to A and the procedure is repeated for the next breath.

During the running period, the automatic control can be turned off and respirator control can be switched to manual control at any time if needed. It should be noted that this system is not designed to mask problems that can occur during mechanical ventilation. For this reason, it has a built-in alarm circuit that produces different alarm signals if ventilation, breathing frequency, pressure, oxygen, or carbon dioxide levels of the patient are outside predefined ranges. These ranges can be redefined in the software for different patients. The controller also safeguards against erroneous measurements of  $\text{CO}_2$  and  $\text{O}_2$  and unsafe levels of ventilation and breathing frequency, as well as gas trapping and intrinsic PEEP and it can communicate with personal computers, printers and other peripheral devices via an RS-232 communication port.

#### The $F_{\text{IO}_2}$ controller

In this study, the closed-loop ventilation controller which automatically adjusts the frequency and tidal volume of breaths of the patient is augmented with a closed-loop control system for automatic adjustment of  $F_{\text{IO}_2}$ . As described earlier, oxygen level of the patient is provided via one of the feedback loops to the ventilation controller to adjust patient's ventilation. However, oxygen supplementation is

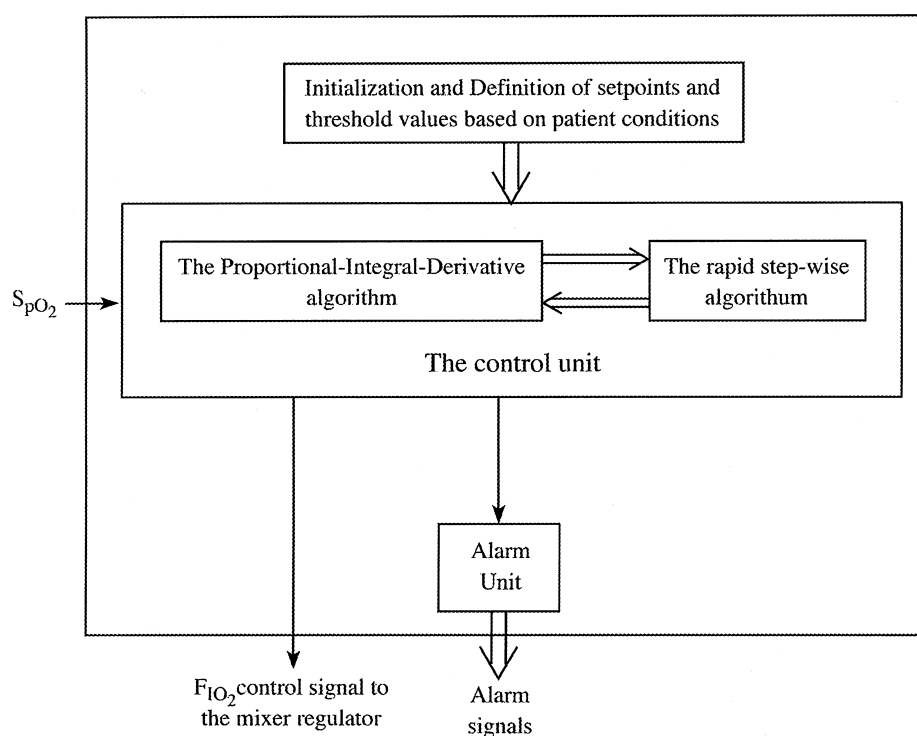


Fig. 3. The schematic diagram of the closed-loop  $F_{IO_2}$  controller.

often necessary in the treatment of patients on mechanical ventilation. In providing the oxygen treatment, it is essential to prevent hypoxemia as well as hyperoxemia and to avoid exposure to toxic levels of oxygen concentration for prolonged periods of time.

In current practice, control of  $F_{IO_2}$  in mechanical ventilation is manual. In this study, a recent technique for automatic adjustment of  $F_{IO_2}$  which is designed to be very sensitive to rapid fluctuations in  $S_{pO_2}$  has been used in combination with the closed-loop ventilation controller [22, 23]. Figure 3 shows the schematic diagram of this closed-loop  $F_{IO_2}$  controller. As can be seen in this diagram, the controller takes feedback of  $S_{pO_2}$  which is measured by using pulse-oximetry, to automatically adjust  $F_{IO_2}$ . At the beginning, based on the conditions of the patient, all the set points and threshold values for  $P_{aO_2}$  and  $S_{pO_2}$  are defined by the medical personnel. The control algorithm takes these values and by using the  $S_{pO_2}$  input from the patient determines the required level of  $F_{IO_2}$  on a breath-by-breath basis. The control algorithm is designed to correct hypoxemia within seconds if  $S_{pO_2}$  falls sharply. This is done by using a fast stepwise control program to respond to rapidly declining levels of  $S_{pO_2}$ . By using this program,  $F_{IO_2}$  is raised stepwise in acute hypoxemia and lowered stepwise as  $S_{pO_2}$  stabilizes, and brought to the safe range. This program interacts with a proportional-integral-derivative

(PID) routine which is designed to provide a fine-tuned, less rapid response to hypoxemia and hyperoxemia when the decline in  $S_{pO_2}$  is not abrupt. By using the combination of the stepwise and the PID algorithms, a rapid robust response to hypoxemia is guaranteed while large fluctuations in  $P_{aO_2}$  as well as hyperoxemia are prevented. The  $F_{IO_2}$  controller has a built-in artifact detector and alarm circuit that protects it against erroneous measurements of  $S_{pO_2}$ . The flow-chart of the control program, the mathematical equations of the system, and the details of its structure and function have been presented elsewhere [22, 23] and are not repeated here for brevity.

#### *Mechanical lung studies*

Figure 4 shows the general description of the equipment set up for the mechanical lung studies. A prototype of the ventilation controller was used in the study. The prototype comprised a Micromint BCC52 microprocessor board, A/D and D/A boards, signal generator and timing control circuits, and an alarm and protection circuit. A separate electronic data simulator network was used to simulate data from the patient and provide them to the ventilation controller as shown in the figure. The controller was connected to a computer monitoring unit via an RS-232



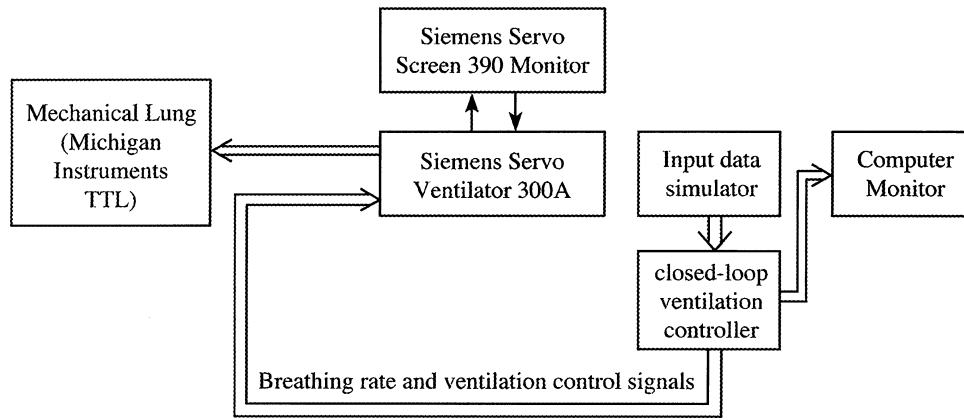


Fig. 4. The general description of the equipment set up for the mechanical lung studies.

communication port. The outputs of the controller were provided to a Siemens Servo Ventilator 300A via an external cable connected to the analog I/O terminal of the ventilator, N81. This was done in order to bypass the manual settings on the front panel of the modified ventilator and control it instead from outside. A Siemens Servo Screen 390 unit was used to monitor the lung mechanics and the outputs of the ventilator. A Michigan Instruments Dual Chamber Training Test Lung (TTL) with variable resistance and compliance was hooked up to the ventilator.

#### Computer simulation studies

The dual closed-loop control system was tested by using computer simulations. In the simulation experiments,  $S_{pO_2}$  was provided to the  $F_{IO_2}$  controller. The output of the  $F_{IO_2}$  controller was applied to an  $O_2$  air mixer, which was simulated by using the following first-order equation:

$$T_1 d F_{IO_2} / dt + F_{IO_2}(t) = G(t) \quad (13)$$

where  $G(t)$  is the control signal applied to the  $O_2$  air mixer and  $T_1$  the time constant of the mixer which was set at 30 s in the experiments. The  $S_{pO_2}$  data along with the patient's lung mechanics and  $CO_2$  data were provided to the closed-loop ventilation controller. The oxygen concentration of the inspired gas and the frequency and tidal volume outputs of the ventilator were automatically controlled. The "patient" was represented by a detailed mathematical model of the human respiratory system [27]. Since the patient's respiration was controlled by the ventilator in these experiments, only the plant was simulated and the respiratory controller of the patient was not included in the mathematical model. The mathematical equations of this model

are described in detail in [27] and are not repeated here for brevity.

The simulation results of this study were obtained by using the block-oriented "Interactive Simulation Language," ISL, on a digital computer under different test conditions.

#### Animal experiments

Six 4–5-month-old Yorkshire pigs weighing 108–132 lb were used in the experiments. All the experiments were carried out in accordance with the standards of the Animal Care Committee at Loma Linda University Medical Center. The pigs were orally intubated with a 7.5 mm endotracheal tube. A 20 gauge angiocath was placed in an ear vein to provide vascular access. A percutaneous arterial catheter was placed in the groin for blood gas measurements. The pigs were sedated and paralyzed with continuous i.v. infusion of Fentanyl 30 mcg/kg/h and Pancuronium Bromide 0.2 mg/kg/h. ECG and pulse oximetry probes were placed. Each animal was placed on the ventilator with both closed-loop controllers active throughout the experiment.

#### Equipment set up for animal experiments

Figure 5 shows a block diagram of the equipment set up for the animal experiments. The equipment composed of a Siemens Servo Ventilator 300A, a Siemens Servo Screen 390 monitor, a BCI9000 capnograph, a HP78534C monitor for ECG and blood pressure, a Nellcor N-200 pulse oximeter, a prototype of the closed-loop ventilation controller, a voltage regulator for adjustment of some of the inputs, a prototype of the  $F_{IO_2}$  controller, a computer hooked up to two closed-loop controllers for inputting data and monitoring, and another computer monitoring system

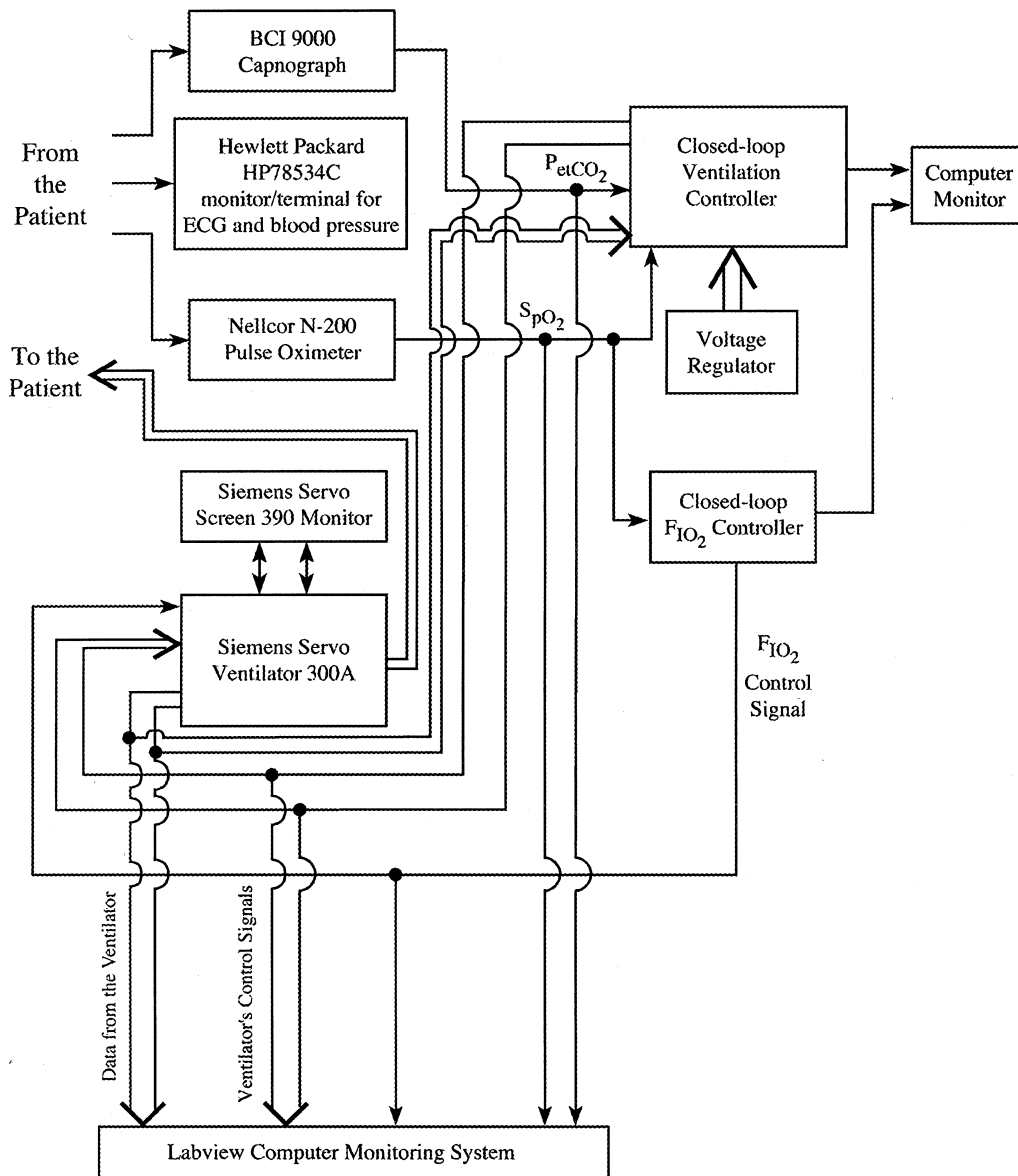


Fig. 5. Block diagram of the equipment set up for the animal experiments.

equipped with LabView software package for recording and analysis of various experimental data.

The ventilator was controlled via an external cable connected to its N81 analog I/O terminal. According to the manufacturer's guidelines, reversible modifications were made to one of the internal PC boards of the ventilator to allow for the external control of the machine. The Siemens Servo Screen 390 monitor was used to monitor the breathing waveforms and the respiratory mechanics data. A BCI9000 capnograph and a Nellcor N-200 pulse oximeter were used to provide the  $P_{etCO_2}$  and  $S_{pO_2}$  data, respectively. These data were inputted to the closed-loop ventilation

controller. The value of  $K_1$ , which represents the difference between  $P_{aCO_2}$  and  $P_{etCO_2}$ , was adjusted periodically by using the voltage regulator unit. The value of  $K_1$  can be used to set the desired  $P_{aCO_2}$  level based on the patient's conditions as is mentioned earlier. In the experiments,  $K_1$  was adjusted by comparing  $P_{etCO_2}$  with  $P_{aCO_2}$  by using periodic blood gas measurements. The values of  $K'$  and  $K''$  were measured by the Siemens Servo Screen 390 monitor and the data were inputted to the ventilation controller. The  $S_{pO_2}$  data measured by the pulse oximeter was also inputted to the closed-loop  $F_{IO_2}$  controller. Both controllers were connected to a computer via RS232 communication

Table 1. Results of the mechanical lung studies

Test	Compliance, $1/K'$ (ml/cmH <sub>2</sub> O)	Resistance, $K''$ (cmH <sub>2</sub> O/l/s)	$\tau = RC$ (s)	PEEP (cmH <sub>2</sub> O)	Measured $V_T$ (l)	Measured $F$ (breaths/min)	$V_E$ (l/min)
Normal	100	7	0.70	0	0.60	12	7.2
COPD	100	16	1.60	0	0.87	7	6.5
COPD	41	38	1.56	5	0.86	7	6.2
Low compliance	37	5	0.18	0	0.43	16	7.0
ARDS	21	9	0.19	8	0.43	15	6.2
ARDS	22	14	0.31	8	0.46	13	6.1
Obstruction + Low compliance	35	19	0.66	5	0.57	11	6.1
Obstruction + ARDS	22	27	0.59	8	0.54	11	6.2
Obstruction + ARDS	21	38	0.80	8	0.59	10	6.0

ports for monitoring the outputs and adjustment of some of the initial data in the software. The control signals were provided to the ventilator via an external cable through the N81 analog I/O terminal of the ventilator. Another computer system equipped with the LabView software package was used to continuously record the experimental data. The transient and steady-state results were obtained and statistical analyses of the data were performed. A  $p$ -value  $< 0.05$  was considered to determine statistical significance.

## RESULTS

### Mechanical lung study results

Table 1 shows the results of the mechanical lung studies. The upper limit pressure of the ventilator was set at 45 cmH<sub>2</sub>O in these experiments. Chronic Obstructive Pulmonary Disease (COPD) was simulated by choosing a high resistance for the mechanical lung and Adult Respiratory Distress Syndrome (ARDS) was simulated by setting low the compliance of the test lung. The Siemens Servo Screen 390 monitor was used to measure the resistance, compliance, the breathing rate and tidal volume of the test lung. In COPD tests, the frequency was low and tidal volume was high whereas in the ARDS simulations the reverse was true. The results show that the controller adjusted the outputs of the ventilator in a manner generally perceived as clinically appropriate.

### Computer simulation results

Figure 6 shows a sample of the simulation results. In Figure 6a, the  $F_{IO_2}$  controller is present but the closed-loop ventilation controller is turned off and conventional ventilation

with fixed values of breathing rate ( $F$ ) of 15 breaths/min and tidal volume ( $V_T$ ) of 0.36 l is applied. The ventilation setting is deliberately chosen to be lower than normal in this test, a condition that can arise easily when the ventilator settings are manually adjusted. In Figure 6b, both closed-loop controllers are present. In both tests, the alveolar-arterial oxygen difference is increased to 25 mmHg to induce hypoxia. The respiratory elastance is 14 cmH<sub>2</sub>O/l and the airway resistance is 8 cmH<sub>2</sub>O/l/s. As shown in 6a,  $P_{aO_2}$  initially falls to 72 mmHg due to the sudden increase in the alveolar-arterial oxygen difference. With the intervention of the  $F_{IO_2}$  controller, hypoxemia is prevented, and  $P_{aO_2}$  stabilizes around 86 mmHg after an initial overshoot to 98 mmHg. In the  $F_{IO_2}$  response, there is a slight initial overshoot to 27% after which it stabilizes around 25% following a few minor oscillations. As seen in the figure, although hypoxemia is prevented with the aid of the  $F_{IO_2}$  controller, but the level of  $P_{aCO_2}$  steadily rises due to lack of sufficient ventilation and reaches about 47 mmHg in about 20 min. In 6b, the test is repeated with the addition of the closed-loop ventilation controller. As can be seen in the figure, there is no initial drop in  $P_{aO_2}$ . In this test,  $P_{aO_2}$  stabilizes around 88 mmHg and  $F_{IO_2}$  oscillates around 22%. Unlike what is seen in Figure 6a, no hypercapnia is observed in Figure 6b and  $P_{aCO_2}$  remains around 39 mmHg throughout the test period. Moreover, a lower  $F_{IO_2}$  value is required for sufficient oxygenation in Figure 6b due to the combined effects of the controllers.

Comparison of these results shows some of the advantages of closed-loop mechanical ventilation versus manual adjustment of  $f$  and  $V_T$ . As shown here, hypercapnia and hypoxemia are both prevented and  $P_{aO_2}$  is regulated in the normal range requiring lower levels of  $F_{IO_2}$  by using the dual closed-loop control system versus using the  $F_{IO_2}$  controller alone. It can also be seen that the

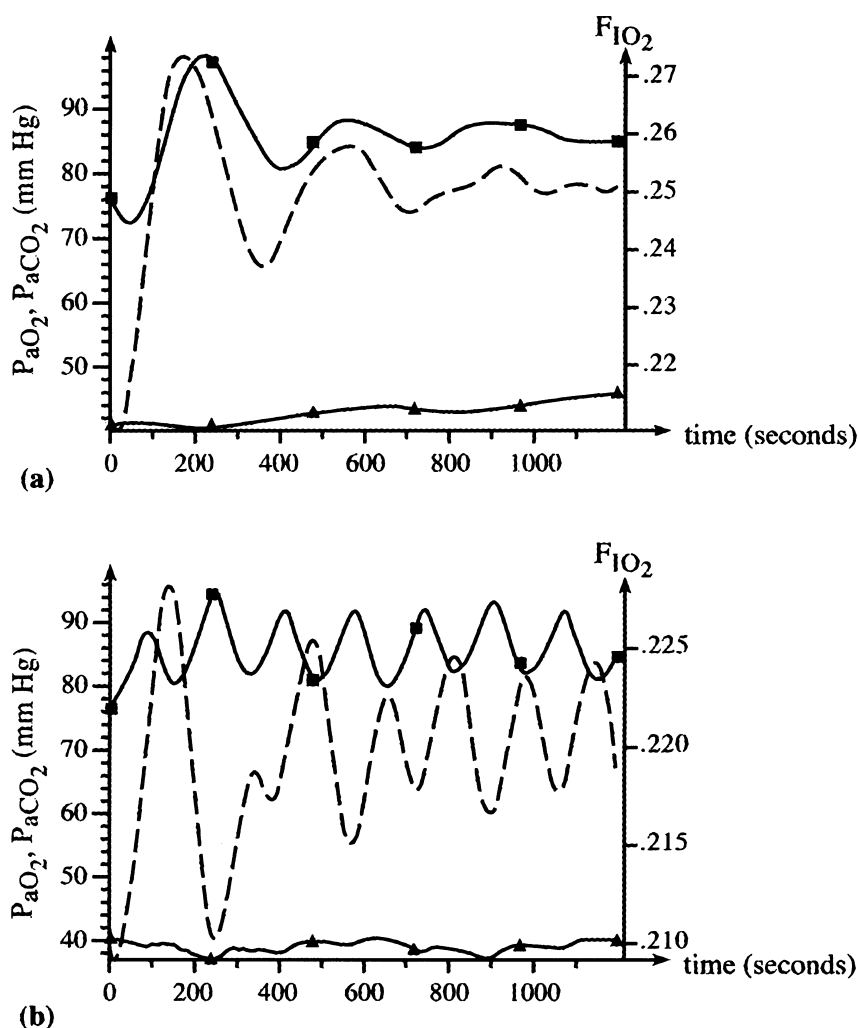


Fig. 6. A sample of computer simulation results. Transient responses of the system to hypoxia. In (a) only the closed-loop  $F_{IO_2}$  controller is used while in (b) the closed-loop ventilation controller is also active. The symbols  $\blacksquare$ ,  $\blacktriangle$  and  $-\cdot-\cdot-$  correspond to  $P_{aO_2}$ ,  $P_{aCO_2}$ , and  $F_{IO_2}$ , respectively.

transient response is shorter and the overall control system is more robust when both closed-loop controllers are present.

#### Results of animal experiments

In the first part of the experiments, which lasted between 45 and 156 min for different animals, the ventilator was set in the VC mode. In the second part, which took 60–142 min, the mode of ventilation was changed to pressure-regulated volume control (PRVC). In each part, the animals were subjected to periods of induced hypoxia, hypercarbia, and apnea. Hypoxia was induced by addition of high concentrations of nitrogen (40%) and thereby diluting the air entering the mixer. Hypercarbia was caused by addition of

carbon dioxide to the inspired gas and apnea was imposed by temporarily disconnecting the animal from the ventilator. Transient as well as steady-state responses were obtained. Blood gas measurements were done intermittently for every 20–40 min.

Two examples of the transient responses are shown in Figures 7 and 8. In Figure 7, the transient responses in hypercarbia are shown. In this test, the ventilator was in the VC mode. As can be seen, despite continuous addition of carbon dioxide (flow of 5 l/min of  $CO_2$  into the air tube) to the inspired gas, there is only a slight rise in  $P_{etCO_2}$  to 39 mmHg at the onset of the test which is brought down to around 36 mmHg in less than 15 s by the intervention of the ventilation controller and the rise in the level of ventilation. The lowered  $P_{etCO_2}$  causes ventilation to decrease

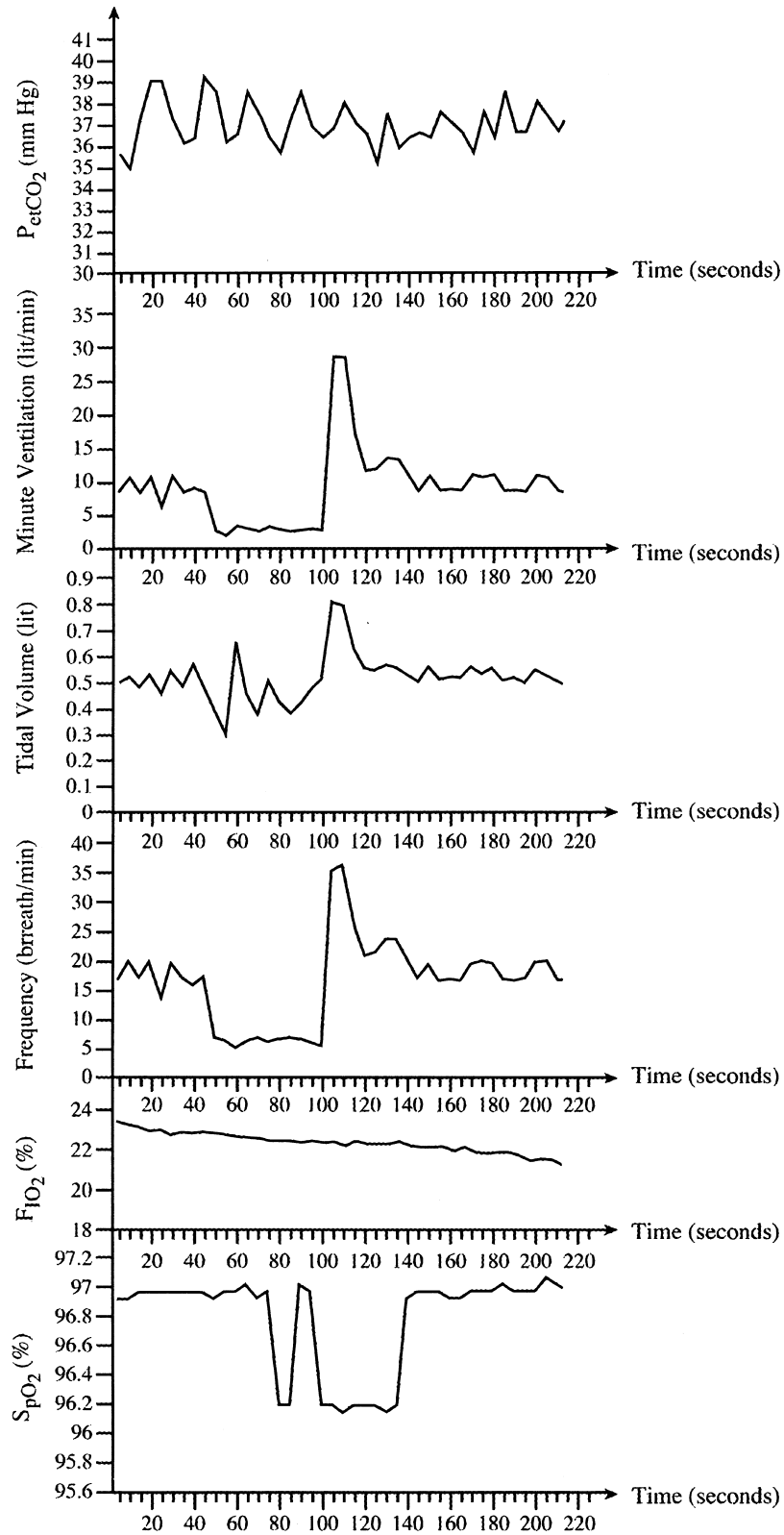


Fig. 7. An example of transient response of the control system to hypercarbia (pig #4).

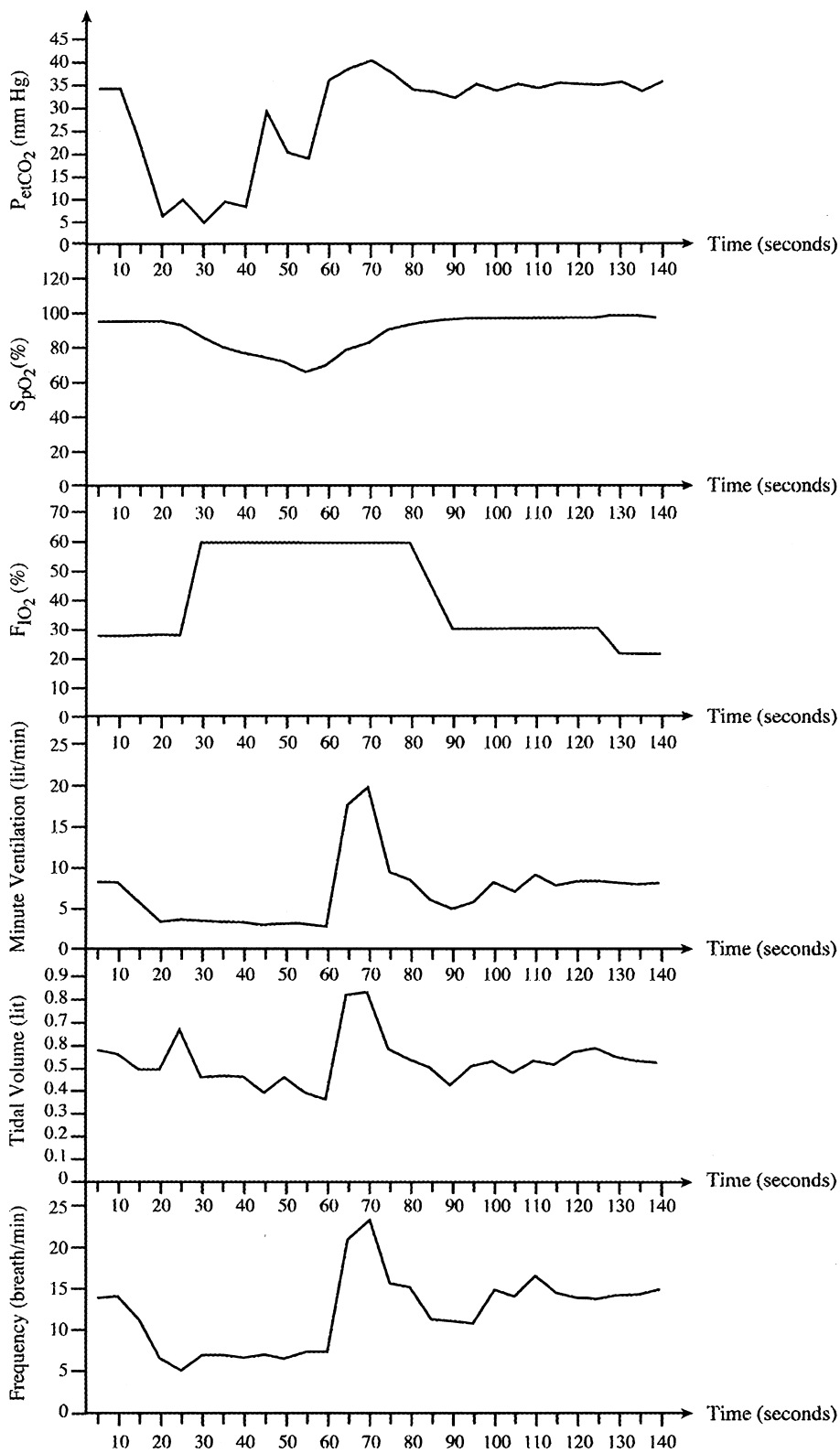


Fig. 8. An example of the response of the control system to imposed apnea (pig #6).

after about 50 s. Then the low values of ventilation cause  $S_{pO_2}$  to decrease and  $P_{etCO_2}$  to increase. The combined effects of high  $P_{etCO_2}$  and low  $S_{pO_2}$  cause a sharp rise in ventilation after about 100 s. Thereafter, the oscillations in  $P_{etCO_2}$  and  $S_{pO_2}$  are reduced and minute ventilation stabilizes around 10 l/min. It should be noted that  $P_{etCO_2}$  remains in the range of 35–39 mmHg and  $S_{pO_2}$  stays above 96% throughout the test while carbon dioxide is continuously added to the inspired gas.  $F_{IO_2}$  falls slightly to about 21.5% by the end of the test period.

Figure 8 shows the transient responses in imposed apnea and shortly thereafter. In this experiment, the ventilator was in the PRVC mode. In this test, while respiratory mechanics along with other input data were used to determine the optimum breathing rate and tidal volume of the breaths, they were also used to automatically adjust the inspiratory pressure for every breathing cycle. As can be seen in Figure 8, at the beginning of the test when apnea is imposed by disconnecting the animal from the ventilator for 40 s,  $S_{pO_2}$  sharply falls to around 65%. During the same time, the reading of the capnometer for  $P_{etCO_2}$  falls due to lack of gas flow. Since the animal was disconnected from the ventilator, the values shown for ventilation, breathing frequency, tidal volume, and  $F_{IO_2}$  in the graphs of Figure 8 during 40 s of apnea were not provided to the animal. After the period of imposed apnea, as soon as the ventilator is connected back to the animal, ventilation sharply rises to about 17 l/min at a frequency of 24 breaths/min, and  $F_{IO_2}$  rises to 60% to correct the induced acute hypoxia. It is seen that both  $S_{pO_2}$  and  $P_{etCO_2}$  are brought back to the normal levels within 20 s of the intervention of the dual closed-loop control system.

The summary of the steady-state results in hypoxia and hypercarbia is shown in Table 2. As shown, the experiments were done by using the VC mode for 45–156 min and the PRVC mode for 60–142 min for different animals. Both closed-loop controllers were used in all experiments. As shown in Table 2,  $S_{pO_2}$  and  $P_{etCO_2}$  were maintained in the normal range all of the time. In hypercarbia experiments, the levels of  $S_{pO_2}$  were higher than those in hypoxia due to higher levels of ventilation. This is true for experiments using the VC as well as the PRVC mode. The blood gas results shown in the last three columns of the table indicate similar results. According to these results, in hypercarbia experiments generally both  $P_{aCO_2}$  and  $P_{aO_2}$  results are higher compared to hypoxia experiments. This is due to high levels of  $CO_2$  in the breathing gas and the resultant higher levels of ventilation.

The values of  $F_{IO_2}$  listed in Table 2 are the oxygen concentrations measured at the output of the  $O_2$  air mixer under steady-state conditions. It should be noted that in hypoxia experiments, the air coming into the mixer was

diluted with high concentrations of nitrogen and the oxygen concentrations at the output of the mixer are the result of addition of the controlled concentrations of oxygen to the diluted air.

The largest standard deviation in hypoxia experiments for  $S_{pO_2}$  under steady-state conditions was  $\pm 1.17\%$  with a mean value of 96.9% while the ventilator was in the VC mode. In these tests, minimum  $S_{pO_2}$  was 95% and it remained above 95.05% most of the time ( $p < 0.05$ ). The largest standard deviation for  $P_{etCO_2}$  in these tests was  $\pm 1.77$  mmHg with a mean value of 39.1 mmHg and the 95% confidence interval of 38.90–39.44 mmHg for the mean value. The blood gas results show that  $P_{aCO_2}$  ranged from 33 to 38 mmHg and  $P_{aO_2}$  ranged between 74 and 126 mmHg in this part of the experiments for different animals.

In the hypoxia experiments, with the ventilator in the PRVC mode, the largest standard deviation for  $S_{pO_2}$  was  $\pm 1.76\%$  with a mean value of 95.37%. The minimum value for  $S_{pO_2}$  was 90.4% in these tests and it remained above 91.2% most of the time ( $p < 0.034$ ). The largest standard deviation in  $P_{etCO_2}$  was  $\pm 1.43$  mmHg with a mean value of 34.87 mmHg and the 95% confidence interval of 34.42–35.32 mmHg for the mean value. The blood gas results show that  $P_{aCO_2}$  in these tests was in the range of 30–38 mmHg and  $P_{aO_2}$  was in the range of 73–102 mmHg for different animals.

In hypercarbia experiments, with the ventilator in the VC mode, the largest standard deviation for  $S_{pO_2}$  was  $\pm 0.46\%$  with a mean value of 97.22%. The minimum  $S_{pO_2}$  in these tests was 96.19% and it remained above 96.5% most of the time ( $p < 0.019$ ). The largest standard deviation for  $P_{etCO_2}$  was  $\pm 1.78$  mmHg with a mean value of 39.17 mmHg, and the 95% confidence interval for mean between 38.9 and 39.44 mmHg. According to the blood gas results, the ranges for  $P_{aCO_2}$  and  $P_{aO_2}$  for different animals were 33–41 and 80–102 mmHg, respectively.

The results of the hypercarbia experiments with the ventilator in the PRVC mode show the largest standard deviation of  $\pm 0.60\%$  for  $S_{pO_2}$  with a mean value of 97.56%. In these tests,  $S_{pO_2}$  was always above 96.2% and remained higher than 96.9% most of the time ( $p < 0.01$ ). The largest standard deviation in  $P_{etCO_2}$  was measured at  $\pm 1.50$  mmHg with a mean value of 39.34 mmHg and the 95% confidence interval for mean of 39.1–39.57 mmHg. The blood gas results show that  $P_{aCO_2}$  ranged from 32 to 39 mmHg and  $P_{aO_2}$  from 74 to 110 mmHg in these experiments for different animals.

According to these results, the dual closed-loop control system maintained  $P_{etCO_2}$ ,  $S_{pO_2}$ ,  $P_{aCO_2}$ , and  $P_{aO_2}$  levels of the animals in the normal range in all the experiments, in the VC as well as the PRVC modes of the ventilator.

Table 2. Summary of steady-state results of the animal studies in hypoxia and hypercarbia

Pig no.	Sex	Tests		Oxygen concentration							Experimental results				
		Weight (lb)	SpO <sub>2</sub> (mean ± SD) (%)	at the mixer output (mean ± SD)	P <sub>et</sub> CO <sub>2</sub> (mean ± SD) (mmHg)	V <sub>E</sub> (mean ± SD) (l)	V <sub>T</sub> (mean ± SD) (l)	F (mean ± SD) (breaths/min)	P <sub>a</sub> CO <sub>2</sub> (mmHg)	P <sub>a</sub> O <sub>2</sub> (mmHg)	pH				
Hypoxia experiments VC ventilation mode															
1	F	120	96.19 ± 0.60	18.14 ± 0.28	39.10 ± 1.77	7.19 ± 1.96	0.54 ± 0.06	13.17 ± 2.47	37	83	7.50				
2	M	128	96.90 ± 1.17	16.07 ± 1.63	33.61 ± 1.00	7.34 ± 1.24	0.52 ± 0.04	14.00 ± 1.33	38	74	7.50				
3	M	132	95.61 ± 0.69	20.54 ± 1.26	32.22 ± 1.36	8.75 ± 1.45	0.54 ± 0.04	16.21 ± 1.90	33	76	7.55				
4	F	118	96.06 ± 0.36	25.61 ± 0.21	36.38 ± 1.29	8.04 ± 1.57	0.49 ± 0.04	16.30 ± 2.19	38	93	7.50				
5	F	126	96.06 ± 0.62	18.22 ± 0.58	33.24 ± 1.45	7.87 ± 1.62	0.55 ± 0.05	14.14 ± 1.93	33	74	7.53				
6	F	108	95.34 ± 0.57	23.06 ± 1.27	34.06 ± 1.53	7.51 ± 1.71	0.51 ± 0.05	14.43 ± 2.28	33	126	7.53				
Hypercarbia experiments VC ventilation mode															
1	F	120	98.16 ± 0.04	18.77 ± 0.09	39.17 ± 1.78	7.17 ± 1.95	0.54 ± 0.06	12.97 ± 2.52	41	82	7.46				
2	M	128	98.13 ± 0.08	18.53 ± 0.08	34.05 ± 1.40	8.30 ± 1.64	0.54 ± 0.04	15.20 ± 2.17	38	84	7.49				
3	M	132	98.09 ± 0.26	18.90 ± 1.11	32.68 ± 1.30	9.45 ± 1.50	0.55 ± 0.03	17.14 ± 1.91	33	89	7.55				
4	F	118	96.63 ± 0.38	19.76 ± 1.24	36.76 ± 1.15	8.59 ± 1.50	0.50 ± 0.04	16.98 ± 2.13	39	102	7.51				
5	F	126	98.09 ± 0.03	18.48 ± 0.09	33.97 ± 1.35	8.94 ± 1.54	0.58 ± 0.05	15.26 ± 1.70	33	80	7.54				
6	F	108	97.22 ± 0.46	22.67 ± 3.21	35.11 ± 1.64	8.50 ± 2.10	0.53 ± 0.05	15.71 ± 2.65	37	101	7.50				
Hypoxia experiments PRVC ventilation mode															
1	F	120	96.21 ± 0.56	18.30 ± 0.28	37.90 ± 1.18	5.87 ± 1.32	0.50 ± 0.05	11.53 ± 1.82	35	73	7.47				
2	M	128	95.37 ± 1.76	15.42 ± 1.35	33.20 ± 1.19	7.27 ± 1.36	0.52 ± 0.04	13.85 ± 1.90	38	68	7.50				
3	M	132	96.06 ± 0.39	23.65 ± 0.57	31.91 ± 1.30	8.39 ± 1.44	0.53 ± 0.04	15.74 ± 1.91	32	85	7.55				
4	F	118	95.47 ± 0.62	21.23 ± 1.54	37.09 ± 0.92	9.27 ± 1.20	0.51 ± 0.03	18.00 ± 1.61	35	80	7.52				
5	F	126	95.62 ± 0.62	22.27 ± 1.34	34.19 ± 1.16	9.57 ± 1.18	0.54 ± 0.03	17.56 ± 1.42	31	78	7.56				
6	F	108	96.02 ± 0.46	24.49 ± 0.61	34.87 ± 1.43	7.83 ± 1.33	0.55 ± 0.05	14.22 ± 1.53	30	102	7.57				
Hypercarbia experiments PRVC ventilation mode															
1	F	120	98.08 ± 0.39	18.76 ± 0.09	39.34 ± 1.50	7.59 ± 1.78	0.56 ± 0.06	13.51 ± 2.17	39	78	7.46				
2	M	128	98.05 ± 0.54	18.49 ± 0.11	34.26 ± 1.44	8.03 ± 1.45	0.54 ± 0.04	14.77 ± 1.91	38	74	7.50				
3	M	132	98.14 ± 0.03	18.98 ± 1.11	32.84 ± 1.28	9.66 ± 1.33	0.55 ± 0.04	17.41 ± 1.60	33	90	7.55				
4	F	118	97.22 ± 0.47	18.66 ± 0.10	37.50 ± 0.87	9.60 ± 1.44	0.52 ± 0.03	18.41 ± 1.92	38	107	7.49				
5	F	126	97.56 ± 0.60	18.56 ± 0.08	34.26 ± 1.16	9.39 ± 1.44	0.54 ± 0.04	17.39 ± 1.72	34	86	7.54				
6	F	108	96.99 ± 0.54	18.72 ± 0.62	35.31 ± 1.42	8.74 ± 1.57	0.56 ± 0.05	15.40 ± 1.81	32	110	7.53				



## DISCUSSION

A dual closed-loop control system for mechanical ventilation is evaluated. In this system, a ventilation controller and an oxygen concentration controller are combined. The breathing frequency, tidal volume, and the inspired fraction of oxygen, are automatically controlled. The closed-loop ventilation controller takes data representing oxygen and carbon dioxide levels of the patient, airway resistance, and respiratory compliance to automatically adjust  $f$  and  $V_T$ . This controller determines  $f$  and  $V_T$  to minimize the respiratory work rate based on a hypothesis by Otis et al. [14]. The  $I:E$  ratio is adjusted by the controller to allow for effective emptying of the lungs in expiration and many other safeguards are provided in the system as explained above.

The closed-loop  $F_{IO_2}$  controller uses feedback of arterial oxygen saturation,  $S_{pO_2}$ , to determine the required level of  $F_{IO_2}$  for every breath. This controller uses the combination of two algorithms to respond to both slow and rapid disturbances in the oxygen balance of the patient. Measurements that look like artifacts are discarded by the dual closed-loop control system and alarms are activated if any artifact or any untoward condition is detected in the patient.

The dual closed-loop control system was tested by using a detailed mathematical model for humans, as well as in mechanical lung studies and animal experimentation. The mechanical lung studies were done to investigate the effect of significantly changing respiratory mechanics. In these tests, the values of respiratory compliance and airway resistance were varied to the extent seen under disease conditions such as severe COPD and ARDS. The animal experiments were performed on six Yorkshire pigs weighing 108–132 lb. In a group of animal experiments, the PRVC mode of the ventilator in which the inspiratory pressure is

adjusted automatically in response to changes in respiratory mechanics, and in another group the VC mode of the ventilator were used in this study. In these tests, hypercapnia and hypoxemia, conditions caused by respiratory insufficiency and disease, were induced by continuously blending high  $CO_2$  concentrations to the inspired gas and by constantly diluting the air entering the mixer by addition of high concentration of nitrogen. Also, in some of the tests, apnea was temporarily imposed to induce hypoxia, and hypercapnia. Pulse oximetry and capnography techniques were used to continuously and noninvasively measure the oxygen and carbon dioxide levels of the patient. Periodic blood gas measurements were done to check and correct the noninvasive measurements and software means were designed and used throughout the experiments to detect and discard measurement artifacts due to pulse oximetry and/or capnography. The respiratory mechanics were measured by using a standard commercial monitor, Siemens Servo Screen 390. The blood gases, the end-tidal partial pressure of  $CO_2$ , and the arterial oxygen saturation levels were maintained in the normal range by the dual closed-loop controller under different disturbances. The analysis of the results showed that the control system responded in less than 25 s to bring the end-tidal partial pressure of  $CO_2$  and the arterial oxygen saturation to the normal safe range.

In conclusion, the results of this study attest to the effectiveness of the proposed dual closed-loop control system under the indicated conditions and show the potential of this control technique to improve ventilatory treatment. However, it should be emphasized that although there are significant similarities between the plant parameters in humans compared to those of the animals tested, there are still some differences that remain to be investigated in future studies.

## GLOSSARY

Symbol	Definition	Unit
$C_1$	Sensitivity factor of the controller to $CO_2$	(mmHg) <sup>-1</sup>
$C_2$	Constant tuning factor	Dimensionless
$C_3$	Constant factor	l
CF	Correction factor for arterial partial pressure of $O_2$	mmHg
$f$	Breathing frequency	breaths/s
$F$	Breathing frequency	breaths/min
$F_{IO_2}$	Inspired fraction of oxygen	Dimensionless
$I:E$	Ratio of inspiration time to expiration time	Dimensionless
$K_1$	Adjustment factor for $CO_2$	mmHg
$K'$	Respiratory elastance (resp. compliance) <sup>-1</sup>	cmH <sub>2</sub> O/l
$K''$	Airway resistance	cmH <sub>2</sub> O/l/sec
MRR	Metabolic rate ratio	Dimensionless

$P_{aCO_2}$	Arterial partial pressure of CO <sub>2</sub>	mmHg
$P_{aO_2}$	Arterial partial pressure of O <sub>2</sub>	mmHg
PEEP	Positive end expiratory pressure	cmH <sub>2</sub> O
$P_{etCO_2}$	End-tidal partial pressure of CO <sub>2</sub>	mmHg
$P_m$	Peak inspiratory pressure	cmH <sub>2</sub> O
$P_{tO_2}$	Transcutaneous oxygen pressure	mmHg
RC	Respiratory time constant	s
$S_{pO_2}$	Arterial oxygen saturation measured by pulse-oximetry	Dimensionless
$\tau$	Respiratory time constant	s
$T_1$	Time constant of the O <sub>2</sub> air mixer	sec.
$V_A$	Alveolar ventilation	l/min
$V_{AR}$	Alveolar ventilation	l/s
$V_C$	Ratio of alveolar ventilation as the net effect of CO <sub>2</sub> to the resting value of ventilation	Dimensionless
$V_D$	The physiologic dead space volume	l
$V_{Dt}$	Total dead space volume including that of the equipment	l
$V_E$	Total ventilation	l/min
$V_{ED}$	Added dead space due to tubes and connections	l
$V_M$	Ratio of alveolar ventilation as the net effect of increase in the rate of metabolism to the resting value of ventilation	dimensionless
$V_{min}$	Minimum allowed tidal volume	l
$V_O$	Ratio of alveolar ventilation as the net effect of oxygen to the resting value of ventilation	dimensionless
$V_T$	Tidal volume	l

## REFERENCES

- Saxton GA, Jr, Myers GH. A servomechanism for automatic regulation of pulmonary ventilation. *J Appl Physiol* 1957; 11: 326–328.
- Frumin MJ, Bergman NA, Holaday DA. Carbon dioxide and oxygen blood levels with a carbon dioxide controlled artificial respirator. *Anesthesiology* 1959; 20(3): 313–321.
- Mitamura Y, Mikami T, Sugawara H, Yoshimoto C. An optimally controlled respirator. *IEEE Trans Biomed Eng* 1971; BME-18: 330–337.
- Coles JR, Brown WA, Lampard DG. Computer control of ventilation and anesthesia. *Med Biol Eng* 1973; 11: 262–267.
- Mitamura Y, Mikami T, Yamamoto K, Mimura K. A dual control system for assisting respiration. *Med Biol Eng* 1975; 13(6): 846–854.
- Coon RL, Zuperku EJ, Kampine JP. Systemic arterial blood pH servo control of mechanical ventilation. *Anesthesiology* 1978; 49(3): 201–204.
- Ohlson KB, Westenskow DR, Jordan WS. A microprocessor based feedback controller for mechanical ventilation. *Ann Biomed Eng* 1982; 10: 35–48.
- Chapman FW, Newell JC, Roy RJ. A feedback controller for ventilatory therapy. *Ann Biomed Eng* 1985; 13: 359–372.
- Ritchie RG, Ernst EA, Pate BL, Pearson JP, Sheppard LC. Closed-loop control of an anesthesia delivery system: Development and animal testing. *IEEE Trans Biomed Eng* 1978; BME-34(6): 437–443.
- Tehrani FT. Method and apparatus for controlling an artificial respirator. U.S. Patent No. 4986268, 22nd January 1991.
- Laubscher TP, Heinrichs W, Weiler N, Hartmann G, Brunner JX. An adaptive lung ventilation controller. *IEEE Trans Biomed Eng* 1994; 41(1): 51–59.
- Schaublin J, Derighetti M, Feigenwinter P, Petersen-Felix S, Zbinden AM. Fuzzy logic control of mechanical ventilation during anesthesia. *Br J Anesth* 1996; 77: 636–641.
- Fernando T, Cade J, Packer J. Automatic control of arterial carbon dioxide tension in mechanically ventilated patients. *IEEE Trans Info Tech Biomed* 2002; 6(4): 269–276.
- Otis AB, Fenn WO, Rahn H. Mechanics of breathing in man. *J Appl Physiol* 1950; 2: 592–607.
- Beddis IR, Collins P, Levy NM, Godfrey S, Silverman M. New technique for servo-control of arterial oxygen tension in preterm infants. *Arch Dis Child* 1979; 54: 278–280.
- Sano A, Kikucki M. Adaptive control of arterial oxygen pressure of newborn infants under incubator oxygen treatments. *Proc IEE* 1985; 132(Part D., No. 5): 205–211.
- Yu C, He WG, So JM, Roy R, Kaufman H, Newell JC. Improvement in arterial oxygen control using multiple model adaptive control procedures. *IEEE Trans Biomed Eng* 1987; BME-34(8): 567–574.
- Morozoff PE, Evans RW. Closed loop control of  $S_{aO_2}$  in the neonate. *Biomed Instr Tech* 1992; 26: 117–123.
- Tehrani FT. A microcomputer oxygen control system for ventilatory therapy. *Ann Biomed Eng* 1992; 20(5): 547–558.
- Tehrani FT, Bazar AR. A feedback controller for supplemental oxygen treatment of newborn infants: A simulation study. *Med Eng Phys* 1994; 16: 329–333.
- Raemer DB, Ji X, Topulos GP.  $F_{IX}$  controller: An instrument to automatically adjust inspired oxygen fraction using feedback control from a pulse oximeter. *J Clin Monit* 1997; 13: 91–101.

22. Tehrani FT. A control system for oxygen therapy of premature infants. *Proc IEEE Eng Med Biol Conf* 2001; 23(2): 2059–2062.
23. Tehrani FT, Rogers M, Lo T, Malinowski T, Afuwape S, Lum M, Grundl B, Terry M. Closed-loop control of the inspired fraction of oxygen in mechanical ventilation. *J Clin Monit Comput* 2002; 17(6): 367–376.
24. Visser BF. Pulmonary diffusion of carbon dioxide. *Phys Med Biol* 1961; 5: 155–166.
25. Riley RL. Gas exchange and transportation. In: Ruch TC, Patton HD, eds. *Physiology and biophysics*. Philadelphia and London: Saunders, 1966: 761–787.
26. Gray JS. *Pulmonary ventilation and its physiological regulation*. Springfield, Illinois: Charles C. Thomas, 1949.
27. Fincham WF, Tehrani FT. A mathematical model of the human respiratory system. *J Biomed Eng* 1983; 5: 125–133.
28. Tehrani FT. Mathematical analysis and computer simulation of the respiratory system in the newborn infant. *IEEE Trans Biomed Eng* 1993; 40(5): 475–481.